MOLECULAR AND CELLULAR BIOLOGY, Jan. 2004, p. 651–661 Vol. 24, No. 2
0270-7306/04/$08.00+0 DOI: 10.1128/MCB.24.2.651–661.2004

Phosphorylation of Critical Serine Residues in Gem Separates Cytoskeletal Reorganization from Down-Regulation of Calcium Channel Activity

Y. Ward,[1] B. Spinelli,[1] M. J. Quon,[2] H. Chen,[3] S. R. Ikeda,[3] and K. Kelly[1]*

Cell and Cancer Biology Branch, Center for Cancer Research, National Cancer Institute,[1] Diabetes Unit, Lab of Clinical Investigation, National Center for Complementary and Alternative Medicine,[2] and Lab of Molecular Physiology, National Institute on Alcohol Abuse and Alcoholism,[3] Bethesda, Maryland 20892

Received 4 September 2003/Returned for modification 8 October 2003/Accepted 23 October 2003

Gem is a small GTP-binding protein that has a ras-like core and extended chains at each terminus. The primary structure of Gem and other RGK family members (Rad, Rem, and Rem2) predicts a GTPase deficiency, leading to the question of how Gem functional activity is regulated. Two functions for Gem have been demonstrated, including inhibition of voltage-gated calcium channel activity and inhibition of Rho kinase-mediated cytoskeletal reorganization, such as stress fiber formation and neurite retraction. These functions for Gem have been ascribed to its interaction with the calcium channel β subunit and Rho kinase β, respectively. We show here that these functions are separable and regulated by distinct structural modifications to Gem. Phosphorylation of serines 261 and 289, located in the C-terminal extension, is required for Gem-mediated cytoskeletal reorganization, while GTP and possibly calmodulin binding are required for calcium channel inhibition. In addition to regulating cytoskeletal reorganization, phosphorylation of serine 289 in conjunction with serine 23 results in bidentate 14-3-3 binding, leading to increased Gem protein half-life. Evidence presented shows that phosphorylation of serine 261 is mediated via a cdc42/protein kinase Cζ-dependent pathway. These data demonstrate that phosphorylation of serines 261 and 289, outside the GTP-binding region of Gem, controls its inhibition of Rho kinase β and associated changes in the cytoskeleton.

The RGK family of small G proteins is structurally unique within the Ras superfamily. The family is composed of Gem (17), Rad (26), Rem (10), and Rem2 (11). The basic structure of the RGK proteins consists of a Ras-related core with COOH- and NH_2-terminal extensions. RGK proteins exhibit significant modifications within the core sequence, suggesting that their mechanism of regulation will be distinct relative to other GTPases. The G3 domain (DXXG), which is conserved among GTPase superfamily members such as elongation factors, G protein α subunits, and Ras superfamily members (4), has been modified to DXWE in RGK proteins. The G3 domain is thought to participate in the binding and hydrolysis of GTP as a result of the invariant aspartate-binding catalytic Mg^{2+} and the amide proton of the invariant glycine forming a hydrogen bond with the γ-phosphate of GTP (21). Consistent with substitution of the glycine residue, the intrinsic GTPase activity of recombinant Gem (7) or Rem (11) appears to be at the border of detection and considerably less than that of Ras.

Another consideration is the inherent flexibility of the Gly residue in the DXXG motif, which appears to be important for allowing a conformational change in the G3 loop and downstream α helix following GTP binding (summarized in reference 4). In Gαs, replacement of Gly with Ala in the G3 region prevents the activation of downstream effectors without preventing binding of GTP (19). Therefore, it is an open question as to whether RGK family members undergo conformational shifts between GDP and GTP bound states similar to other GTPases.

Other mechanisms of regulation related to unique structural features of the RGK proteins likely exist. RGK family members contain carboxyl extensions of approximately 40 amino acids. These extensions contain a calmodulin binding site (12, 20) and a perfectly conserved terminal sequence of 10 amino acids. Phosphorylations of the carboxyl extensions of Gem (17, 20), Rad (20), and Rem (9) have been described. In addition, the COOH terminus of Rem has been reported to bind 14-3-3 (9), although the specific binding site was not determined. Amino-terminal extensions are more variable in length and sequence among the family members. Finally, unlike most Ras superfamily members, at least some RGK proteins appear to be regulated at the level of protein expression. Gem is an early response gene that is dramatically regulated at the transcriptional level (17), and Rad protein levels are regulated by post-translational processes (32).

Recent advances in defining functional assays for Gem have made it possible to begin addressing the regulation of this RGK protein. The development of cell-based assays has followed from the separate descriptions of two Gem-binding proteins, the voltage-gated calcium channel β subunits (3) and Rho kinase β (30). Both proteins bind Gem within the core region. Gem down-regulates voltage-gated calcium channel activity, which exists mainly in neuronal and endocrine cells (3). One mechanism that has been suggested is that Gem binds and sequesters the β subunit, resulting in inhibition of α-subunit expression at the plasma membrane (3).

Gem is also expressed in cell types that do not express voltage-gated calcium channels, and a role for Gem in regu-

* Corresponding author. Mailing address: Building 10, Room 3B43, CCR, NCI, NIH, Bethesda, MD 20892. Phone: (301) 435-4652. Fax: (301) 435-4655. E-mail: kkelly@helix.nih.gov.

lating cytoskeletal alterations has been observed in various cell types (1, 16, 23). In addition to ROKβ, Gem has been shown to bind KIF-9, a kinesin-like protein (23), and Gmip, a RhoGAP-containing protein (1). Whether KIF-9 or Gmip affects cytoskeletal morphology and the role of Gem in regulating these proteins is yet to be established. Gem regulation of cytoskeletal alterations mediated by ROKβ has been demonstrated. Ectopic Gem expression inhibits ROK-mediated formation of stress fibers, focal adhesions, and neurite retraction (30). Consistent with inhibiting endogenous ROKβ, Gem stimulates neurite extension and cell flattening in neuroblastoma cells (16). Gem inhibits the ability of ROKβ to phosphorylate myosin light chain and myosin phosphatase, but not LIM kinase, suggesting that the ROKβ-Gem interaction blocks the interaction of ROK with specific substrates (30). Because cytoskeletal function is involved in the intracellular transport of surface-bound receptors (27), one question has been whether calcium channel β subunits and ROK represent entirely separate effector pathways or whether they might exist together in a supramolecular complex.

Here we show that serine-to-alanine point mutations in serines 261 and 289 within the COOH terminus of Gem, outside the Ras-related GTP-binding core and ROKβ-binding domain, lead to a complete loss of Gem-mediated cytoskeletal reorganization. By contrast, inhibition of voltage-gated calcium channel activity is unaffected by these same mutations but instead is reversed in GTP- and calmodulin-binding mutants. Thus, pathways affecting calcium channels and Rho kinase appear to be separable. Data presented suggest that COOH-terminal phosphorylation, in addition to regulating cytoskeletal function, results in a conformational change that is stabilized by bidentate 14-3-3 binding, leading to an increased half-life for the phosphorylated Gem protein.

MATERIALS AND METHODS

Antibodies. The anti-14-3-3β (K-19) antibody used for Western blot analysis was obtained from Santa Cruz Biotechnology (Santa Cruz, Calif.). The anti-Gem polyclonal 270 PS and anti-Gem monoclonal P2D10 antibodies have been previously described (16, 17). The anti-phospho Gem peptide antibodies were produced as follows. The peptide containing phosphoserine 261, NH_2-QKRKE(pS)MPRKARC-COOH, was synthesized by United States Biological (Swampscott, Mass.). The peptides were conjugated with McKLH using the Imject maleimide-activated immunogen conjugation kit (Pierce, Rockford, Ill.) and sent to Spring Valley Laboratories, Inc. (Sykesville, Md.) for rabbit antibody production. The peptide containing phosphoserine 289, NH2-MAFKLKSK(pS)CHDC-COOH, was synthesized by Biosynthesis (Lewisville, Tex.), and the rabbit polyclonal antibody was produced by SAIC (Frederick, Md.). Affinity purification of the antibodies was performed with *N*-hydroxysuccinimide-activated Sepharose 4 (Pharmacia Biotech) linked to the peptide. The anti-phospho 261 and anti-phospho 289 antibodies were used for Western blot analysis at a concentration of 1:200 and 1:500, respectively.

Inhibitors. The kinase inhibitors Go6976, Go6850, H9 dihydrochloride, KT5720, PD98059, and KN93 were purchased from Calbiochem (San Diego, Calif.). W7 was from Biomol Research Laboratories, Inc. (Plymouth Meeting, Pa.), LY294002 was from Biosource International, Inc. (Camarillo, Calif.), and Y27632 was from Welfide Corp. (Tokyo, Japan). KT5823 and Apigenin were provided by Alexis Biochemicals (San Diego, Calif.).

Plasmids. A QuickChange site-directed mutagenesis kit (Stratagene, LaJolla, Calif.) was used to generate the mutants of Gem in pMT2T and pRC-CMV vectors. Mutagenized inserts were verified by sequence determination. A dominant inhibitory phosphatidylinositol 3-kinase (PI 3-kinase) regulatory subunit, p85(Δ479-513), was described previously (24). Constitutively active protein kinase Cζ (PKCζ) was generated by mutating Ala 119 to Asp in the pseudosubstrate region (28). PKCζ kinase dead is a mutation of Leu 281 to Trp (25). Wild-type phosphoinositide-dependent kinase-1 (PDK-1) and kinase-inactive PDK-1(K114A) have been described elsewhere (5).

Transfections, immunoprecipitations, and Western blot analysis. Cos-7 cells were plated at 2.0×10^6 cells/10-cm cell culture plate in Dulbecco's modified Eagle's medium containing 10% fetal bovine serum. Cells were transfected with 4 μg of total DNA using Lipofectamine Plus following the Invitrogen protocol. Soluble protein extracts were prepared as previously described (16) with the addition of 4 nM calyculin, 25 mM β-glycerophosphate, and 10 mM NaF. The extract was precleared on 50 μl of recombinant protein G-agarose beads (Invitrogen) for 30 min at 4°C, followed by an incubation of the precleared lysate with 25 μl of packed beads (per sample) and 12 μg of anti-Gem monoclonal antibody P2D10 for 2 to 4 h at 4°C. Beads were then washed three times in lysis buffer, resuspended in sodium dodecyl sulfate-polyacrylamide gel electrophoresis (SDS-PAGE) sample buffer, and boiled for 2 min. SDS-PAGE gels were run and electroblotted onto polyvinylidene difluoride membranes, and Western blot analysis was performed.

Calmodulin binding. To perform the calmodulin-binding experiments, cells were transfected, harvested 48 h later, and lysed as described above. The cellular extract was precleared on glutathione-Sepharose 4B beads (Amersham Bioscience, Piscataway, N.J.) for 30 min at 4°C. The precleared extract was subsequently incubated with 25 μl of packed calmodulin-Sepharose 4B beads (Amersham Bioscience) for 4 h at 4°C. The beads were then washed three times with lysis buffer, resuspended in SDS-PAGE sample buffer, and boiled for 2 min. Western blot analysis was performed with anti-Gem polyclonal antibodies.

Electrophysiology of dissociated SCG neurons. Single superior cervical ganglion (SCG) neurons were isolated from 10- to 14-week-old male Wistar rats as previously described (14). A mammalian expression vector pRC-CMV containing the wild-type or mutant GEM cDNA (0.1 μg/μl in 10 mM Tris [pH 8]) was injected into the nucleus of SCG neurons 4 to ~8 h following cell isolation with an Eppendorf FemtoJet microinjector and a 5171 micromanipulator (14). Neurons were coinjected with enhanced green fluorescent protein (EGFP) cDNA (5 ng/μl; pEGFP-N1; Clontech Laboratories, Palo Alto, Calif.) to facilitate later identification of successfully injected cells. Neurons were used for recording 20 to 24 h after injection.

Whole-cell currents were recorded with a patch-clamp amplifier (Axopatch 200B; Axon Instruments) at room temperature (21 to ~24°C) using the conventional variant of the patch-clamp technique (13) as previously described (15). For recording calcium current, patch electrodes were pulled from borosilicate glass capillaries (Corning 7052; Garner Glass, Claremont, Calif.) on a P-97 Flaming-Brown micropipette puller (Sutter Instruments, Midland, San Rafael, Calif.), fire polished on a microforge, and filled with a solution containing 120 mM *N*-methyl-D-glutamine, 20 mM tetraethylammonium-OH, 10 mM HEPES, 11 mM EGTA, 1 mM $CaCl_2$, 14 mM Tris-creatine phosphate, 4 mM Mg-ATP, and 0.3 mM Na_2-GTP; pH was adjusted to 7.24 with methanesulfonic acid and HCl (final Cl^- concentration of 20 mM). Pipette resistance ranged from 1 to 3 MΩ, yielding uncompensated series resistances of 2 to 6 MΩ. Series resistance compensation of 80% was used in all recordings. The external solution consisted of 145 mM tetraethylammonium methanesulfonate, 10 mM HEPES, 15 mM glucose, 10 mM $CaCl_2$, and 300 nM tetrodotoxin (pH 7.35 and 320 mosmol/kg). Voltage protocol generation and data acquisition were performed using custom data acquisition software on a Macintosh computer with an ITC-18 interface board (InstruTECH, Port Washington, N.Y.). I_{ca} traces were low pass filtered at 2 to 5 kHz and digitized at 10 kHz. For I_M recordings, pipettes were pulled from borosilicate glass capillaries (1B150F-4; World Precision Instruments, Sarasota, Fla.) and filled with a solution consisting of 140 mM KCl, 0.1 mM EGTA, 10 mM HEPES, 4 mM Mg-ATP, 0.1 mM Na_2-GTP, 0.1 mM Tris-creatine phosphate (pH adjusted to 7.25 with KOH; 300 mosmol/kg). The external solution contained 150 mM NaCl, 2.5 mM KCl, 10 mM HEPES, 1 mM $MgCl_2$, 1 mM $CaCl_2$, 15 mM glucose, 300 nM tetrodotoxin (pH adjusted to 7.35 with NaOH; 325 mosmol/kg). I_M traces were low pass filtered at 1 kHz and digitized at 2 kHz. Drugs were applied by positioning a silica tube (inner diameter, 200 μm) of a custom-designed gravity-fed microperfusion system at ~100 μm from the cell. Oxotremorine-M (OXO-M) and norepinephrine were purchased from Sigma (St. Louis, Mo.).

Ca^{2+} current traces and current-voltage relationships were corrected for linear leakage current as determined from hyperpolarizing pulses. I_{ca} amplitude was determined 10 ms after the onset of a test pulse. M current traces were not leak subtracted. Numerical values are expressed as the mean ± the standard error of the mean (SEM). Statistical comparisons were made by using Student's *t* test or analysis of variance followed by Dunnett's test. The differences were considered significant if P was ≤ 0.05.

T-cell activation. Human T cells were plated (3.0×10^6 cells/10-cm cell culture plate) in RPMI 1640 medium with 10% fetal bovine serum. Cells were stimulated

with the addition of 20 ng of phorbol myristate acetate/ml and 5 μg of phytohemagglutinin (Sigma)/ml and incubated for various times. Three plates of each time point were combined, washed with phosphate-buffered saline (PBS), and analyzed for Gem protein using the immunoprecipitation and Western blotting protocols described above.

Immunofluorescence. Exponentially growing HeLa cells were plated on glass coverslips (A. Daigger & Co.) in 24-well cell culture dishes and incubated overnight. The following day, cells on each coverslip were transfected with 0.5 μg of PMT2T-Gem, using Lipofectamine Plus (Invitrogen Life Technologies). Cells were then fixed with 4% paraformaldehyde for 10 min at room temperature, rinsed three times with PBS, and permeabilized with 1% Triton X-100 in 0.2% bovine serum albumin (BSA)–PBS for 2 min at room temperature. Cells were stained using polyclonal anti-Gem antibody followed by antivinculin monoclonal antibody staining as described previously (30). Stained cells were examined on a Zeiss Axioplan microscope equipped with a 100×/1.4 oil immersion objective, and confocal images were generated on a Zeiss LSM 510.

Neuroblastoma neurite extension assay. Neurite remodeling resulting from transfection of N1E-115 murine neuroblastoma cells with Gem or Gem mutants was assayed as described previously (16). Transfections were done using Lipofectamine Plus.

PC12 cell culture and transfection. PC12 cells were maintained in Dulbecco's modified Eagle medium supplemented with 7.5% heat-inactivated fetal bovine serum and 7.5% heat-inactivated horse serum at 37°C and 5% CO_2. Cells were plated on collagen IV-coated six-well cell culture dishes (BD Biosciences) at a concentration of 10^6 cells per well. Twenty-four hours later, cells were transiently transfected with 8 μg of PMT2T-based expression plasmid and 2 μg of PCDNA3-hGH using Lipofectamine 2000 (Invitrogen Life Technologies). Twenty-four hours following transfection, PC12 cells were fed with fresh culture medium and incubated overnight at 37°C and 5% CO_2. Forty-eight hours following transfection, PC12 cells were rinsed twice with physiological salt solution (PSS) containing 20 mM HEPES (pH 7.4), 140 mM NaCl, 5 mM KCl, 2.5 mM $CaCl_2$, 1 mM $MgCl_2$, 1 mM KH_2PO_4, 10 mM glucose, and 0.1% BSA. Cells were preincubated in PSS for 30 min. Nonstimulated secretion was investigated by incubating PC12 cells in PSS for another 30 min, while depolarization-induced secretion was shown by incubating cells for 30 min in a high-KCl solution containing 20 mM HEPES (pH 7.4), 65 mM NaCl, 80 mM KCl, 2.5 mM $BaCl_2$, 1 mM $MgCl_2$, 1 mM KH_2PO_4, 10 mM glucose, and 0.1% BSA. Growth hormone protein concentration was determined by Western blot analysis of cell-conditioned medium using polyclonal anti-human growth hormone (hGH) antibody obtained from A. F. Parlow (NIDDK National Hormone and Peptide Program). To determine the cellular hGH, at the end of the incubations cells were lysed in 25 mM HEPES (pH 7.4), 10% glycerol, 1% Triton X-100, 150 mM NaCl.

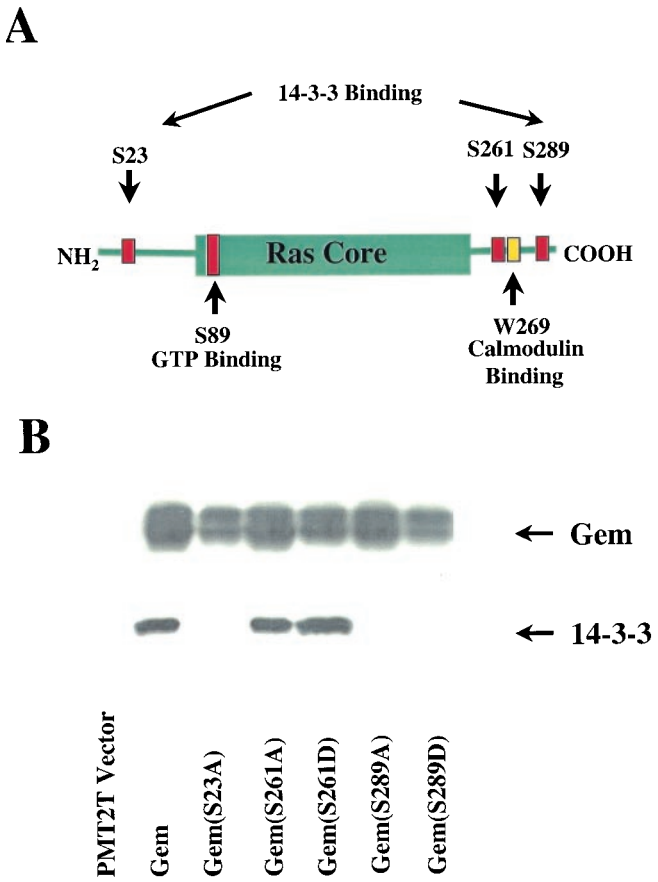

FIG. 1. Interaction of Gem and 14-3-3. (A) The positions of serines subjected to mutagenesis in Gem are shown relative to the ras core, 14-3-3 binding site, and calmodulin binding site. (B) Cos-7 cells were transfected with wild-type or mutant Gem. Cell lysates were immunoprecipitated with anti-Gem monoclonal antibody and, subsequently, coprecipitated 14-3-3 was detected by Western blot analysis using anti-14-3-3β polyclonal antibody. Total Gem expression in the cell lysates was determined by Western blotting with anti-Gem polyclonal antibody.

RESULTS

Mapping the 14-3-3 binding sites in Gem. As an approach to identifying regulators and effectors of Gem, our investigators previously used full-length Gem as bait in a yeast two-hybrid analysis of a Raji B-cell library (30). Clones encoding 14-3-3β were isolated multiple times. Following immunoprecipitation of Gem from extracts of transiently transfected Cos-7 cells, 14-3-3 was detected in Western blotting (Fig. 1B), confirming the interaction of Gem and 14-3-3 in mammalian cells. A Gem construct with the COOH-terminal 34 amino acids deleted (amino acids 263 to 296) no longer bound 14-3-3 in a *Saccharomyces cerevisiae* two-hybrid analysis (data not shown). In order to determine the 14-3-3 binding site, we introduced separate serine-to-alanine mutations at positions 261, 287, 289, and 294 (Fig. 1A and data not shown). Extracts from Cos-7 cells transfected with the various mutants of Gem were analyzed for the coassociation of Gem and 14-3-3. As shown in Fig. 1B, mutation of serine 289 resulted in a loss of 14-3-3 binding. The sequence surrounding serine 289, KSKpSCH, is not a consensus 14-3-3 binding site. Although serine 261 is located within a consensus 14-3-3 binding site, RXXpSXP, it was not involved in 14-3-3 binding.

14-3-3 exists as a dimer, and many 14-3-3 target proteins require two phosphorylation sites to stably bind 14-3-3. An analysis of RGK family members suggested another possible 14-3-3 binding site in Gem. The COOH-terminal binding site that includes serine 289 is found in Rad, Rem, and Rem2. Although the binding sites were not determined, it has been reported that Rem but not Rem2 binds 14-3-3 (9). Rem2 has a truncated amino terminus, missing between 33 and 39 amino acids relative to the other family members and, therefore, we considered this region as possibly significant in determining 14-3-3 binding. Serine 23 within this region in Gem was mutated to alanine, resulting in the loss of 14-3-3 binding (Fig. 1B). Serine 23 is contained within the sequence RWpSIP, which meets the requirement for a weak consensus 14-3-3-binding sequence by having a proline at the +2 position. In conclusion, the stable interaction of Gem and 14-3-3 requires binding of 14-3-3 with two phosphoserine binding sites in Gem, one within the N-terminal extension and one within the C-terminal extension.

In order to address whether Gem binds specific isoforms of 14-3-3, we determined the coassociation of Gem and 14-3-3 in

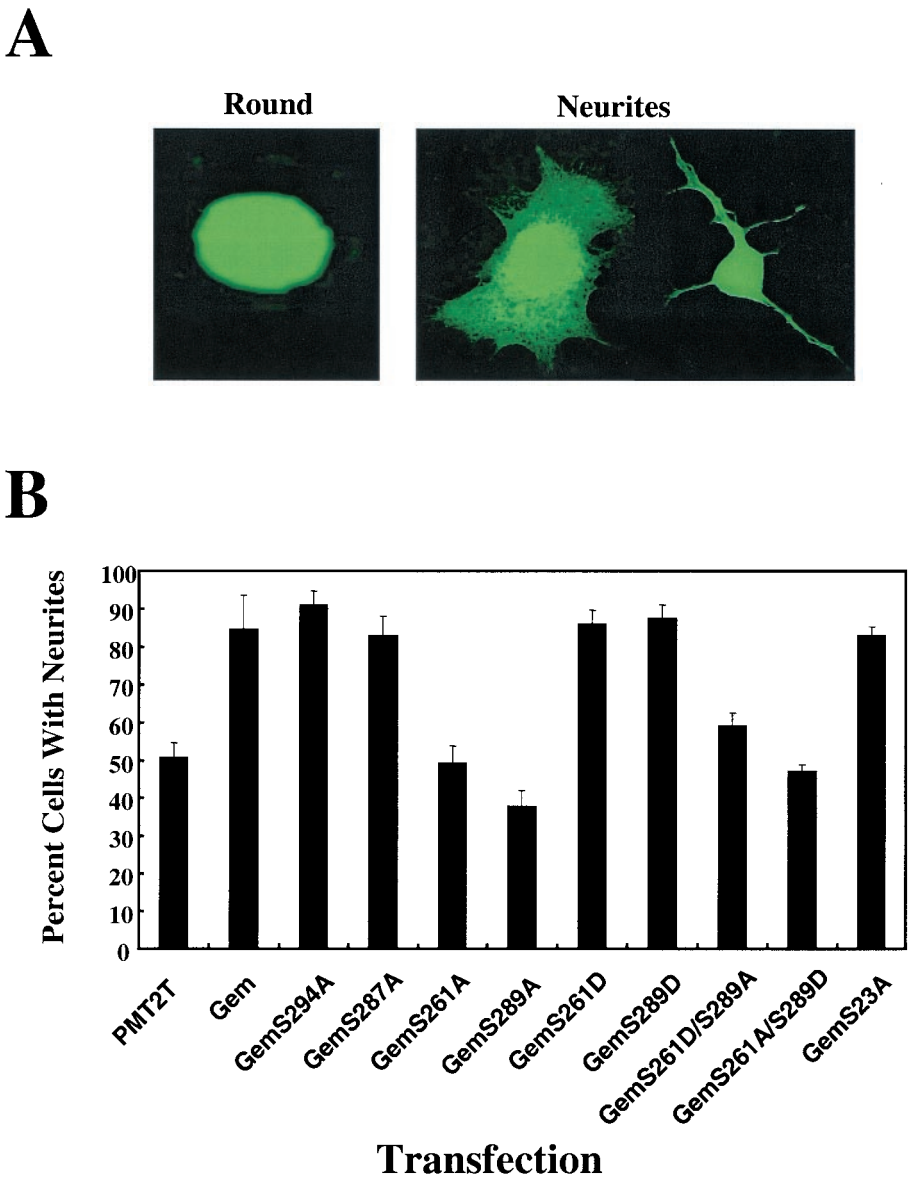

FIG. 2. (A) Representative morphologies of N1E-115 cells. Gem stimulates cell flattening and neurite extension. (B) Effects of Gem and Gem mutants on neurite extension in N1E-115 murine neuroblastoma cells. Cells were cotransfected with pEGFP-N1 and Gem plasmids as indicated. The percentage of transfected cells with neurites is shown (from an average of five independent experiments) with standard deviations. Mutation of serine 261 or 289 to alanine inhibits the cytoskeletal effects of Gem. (C) Effects of Gem and Gem mutants on focal adhesion dissolution. HeLa cells were transfected with empty vector and pEGFP-N1 or various Gem cDNAs. Gem-expressing cells were stained with anti-Gem polyclonal antibody followed by an anti-rabbit fluorescein isothiocyanate-conjugated antibody and antivinculin monoclonal antibody followed by an anti-mouse rhodamine-conjugated secondary antibody. Cells expressing empty vector and GFP were stained for vinculin only. The percent transfected cells containing focal adhesions throughout the cell surface was quantified in three independent experiments. Four hundred cells were counted for each. (D) Confocal images showing representative focal adhesion patterns.

the neuroblastoma cell line SY5Y. Western blotting was performed on Gem immunoprecipitates using isoform-specific antibodies to 14-3-3. 14-3-3ζ, -γ, -τ, and -β were observed to bind to Gem (data not shown). Therefore, no specificity was apparent for the binding of these 14-3-3 isoforms to Gem.

Phosphorylation of serines 261 and 289 is required for Gem-mediated neurite extension in N1E-115 cells. Our investigators have shown that Gem stimulates cell flattening and neurite extension in NIE-115 cells (reference 30 and Fig. 2A) and opposes Rho kinase β-mediated cell rounding, a function that is dependent upon the interaction of Gem and ROKβ. In order to determine whether phosphorylation of serines 261, 287, 289, or 294 in the COOH-terminus affects such function, we tested the appropriate serine-to-alanine Gem mutations for their ability to stimulate flattening and neurite extension in transfected N1E-115 cells (Fig. 2B) and opposition to ROKβ-stimulated neurite retraction (data not shown). Interestingly, mutation of either serine 289 or serine 261 to alanine inhibited the

C

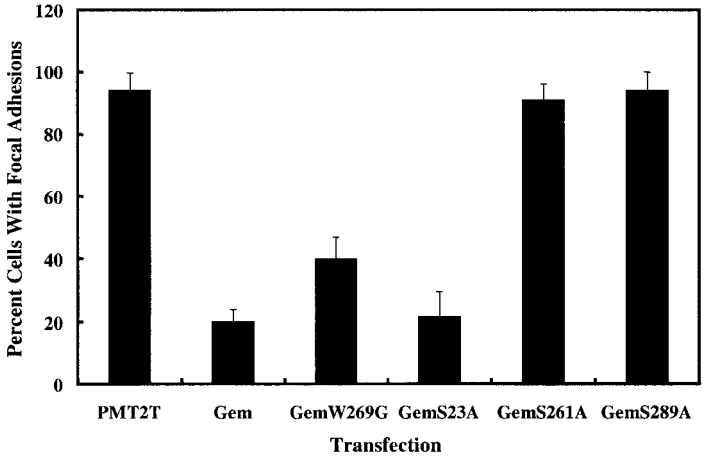

D

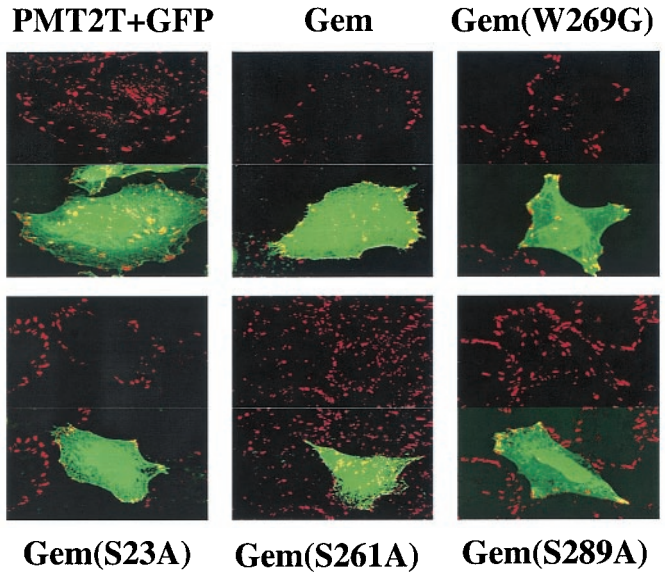

FIG. 2—*Continued.*

morphological activity of Gem, whereas mutation of serines 287 and 294 had no effect (Fig. 2B). In order to mimic the structure of phosphoserine, serines 261 and 289 were mutated to aspartic acids. Both of these mutants stimulated neurite extension (Fig. 2B) and opposed ROKβ (data not shown) similarly to wild type. To determine whether mimicking constitutive phosphorylation with aspartic acid at one site (serine 261 or 289) could overcome the lack of phosphorylation at the other site, the double mutants Gem261D289A and Gem261A289D were assayed in the N1E-115 system. Neither mutant showed activity, suggesting that both sites need to be phosphorylated or modified with a negative charge to stimulate neurite extension.

The cytoskeletal-reorganizing activity of Gem correlates with phosphorylation of serine 289 but not 14-3-3 binding. Because phosphorylation of serine 289 correlated with both neurite extension activity and 14-3-3 binding, we determined whether 14-3-3 binding was necessary for this function. GemS23A, which does not bind 14-3-3, was assayed in N1E-115 cells and found to have activity similar to wild-type Gem (Fig. 2B), suggesting that 14-3-3 binding is not necessary for neurite extension activity. Consistent with this, GemS289D did not bind 14-3-3 but was functional (Fig. 1B and 2B). This suggests that activity mediated through ROKβ binding to Gem requires a negative charge on serine 289, perhaps leading to a necessary conformational change. By contrast, 14-3-3 binding

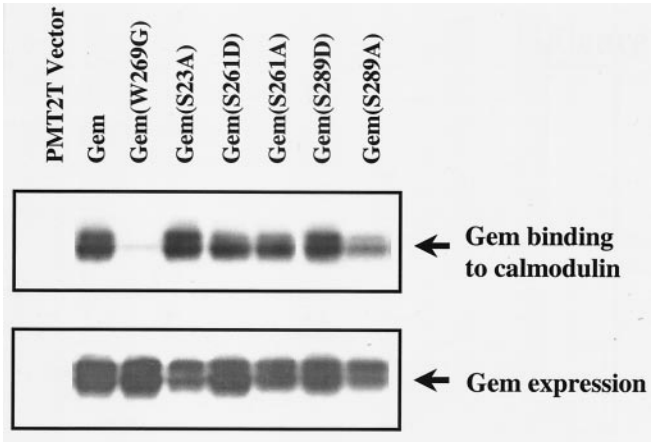

FIG. 3. Calmodulin binding to Gem is independent of phosphorylation at serine 261 or 289. Lysates from Cos-7 cells transfected with wild-type or mutant Gem were incubated with calmodulin-Sepharose beads. Calmodulin-bound Gem and total Gem expressed were identified by Western blot analysis using anti-Gem polyclonal antibody.

to phosphoserine 289 appeared to be more stringent, possibly as a result of direct contact of 14-3-3 and Gem at phosphoserine 289. Another consequence of Gem overexpression on cytoskeletal reorganization is loss of focal adhesions, but not of peripheral focal contacts (30). The above mutant forms of Gem were assayed for their ability to stimulate focal adhesion dissolution (Fig. 2C and D). The results paralleled those observed in the N1E-115 neurite extension assay, demonstrating further that tandem phosphorylation of serines 261 and 289 in Gem is required for ROKβ-dependent cytoskeletal reorganization. In addition, the calmodulin-binding mutant GemW269G (see below) was assayed for its effect on focal adhesions and was found to have activity similar to wild type, demonstrating that calmodulin binding is not required for Gem cytoskeletal function.

Neither phosphorylation of serine 261 nor of 289 influences calmodulin binding. Gem binds calmodulin in the COOH terminus, between serines 261 and 289. To test whether serine phosphorylation and/or 14-3-3 binding affects calmodulin binding, the ability of various Gem mutants to bind calmodulin-Sepharose was determined. A mutation from tryptophan to glycine at position 269 in mouse Gem (or the equivalent position 270 in human Gem) within the helix that binds calmodulin inhibits its binding. Here, the calmodulin-binding mutant is labeled GemW269G to remain consistent with the published literature (3, 12). As shown in Fig. 3, with the exception of GemW269G, the various mutants bound calmodulin-Sepharose. Therefore, phosphorylation at either site 261 or 289 within the COOH terminus is not required for nearby calmodulin binding.

Inhibition of voltage-gated calcium channels by Gem requires GTP and calmodulin binding, but not phosphorylation of serine 261 or 289. To test the effects of Gem isoforms (wild type and point mutants) on neuronal voltage-activated Ca^{2+} channels, we expressed Gem constructs in rat sympathetic neurons (derived from the SCG) by intranuclear microinjection. The majority of I_{Ca} in these neurons arises from $Ca_V2.2$, or N-type, Ca^{2+} channels. Representative current-voltage relationships and I_{Ca} traces (inset) from a control (uninjected) and Gem cDNA-injected neuron are shown in Fig. 4A. Recordings made approximately 24 h following injection revealed a dramatic decrease in I_{Ca} amplitude across the voltage range examined (ca. −30 to +80 mV) with no apparent alteration in current kinetics. Although not studied in detail, the residual I_{Ca} recorded following Gem expression displayed a similar current-voltage relationship and modulation by norepinephrine (approximately 60% inhibition [data not shown]) as control I_{Ca}. The effects of Gem wild type and mutant expression were quantified by determining I_{Ca} density (peak I_{Ca} amplitude normalized to membrane capacitance [pA/pF]) for each condition. As summarized in Fig. 4B, mean I_{Ca} density in neurons injected with wild-type, S261A, or S289A Gem cDNA was greatly reduced when compared with uninjected neurons or neurons expressing only EGFP (data not shown). Conversely, injection of Gem S89N or W269G cDNA did not significantly reduce mean I_{Ca} density. Thus, mutations which disrupt GTP and calmodulin binding diminish the ability of Gem to reduce I_{Ca} density, whereas mutations that alter the phosphorylation potential of residues 261 or 289 have no significant effect on this ability. It should be noted that the W269G mutation produced a partial reduction in I_{Ca} density that did not reach a level of significance ($P = 0.11$, one-way analysis of variance and Newman-Keuls test). Since single neuron expression levels could not be evaluated, it is possible that this construct has a significant effect at higher levels of expression or with increased trials.

The ability of Gem to alter the function of an ion channel unrelated to Ca^{2+} channels was determined to assess the specificity of the aforementioned effects. Figure 4C depicts representative M-current (I_M) traces recorded from control (left) and Gem-injected (right) SCG neurons. I_M is a noninactivating K^+ current that is activated by voltage and readily modulated by a variety of neurotransmitters but otherwise shares little similarity with I_{Ca}. I_M amplitude, kinetics, and modulation by the muscarinic acetylcholine receptor agonist OXO-M were examined during a 0.5-s voltage pulse to −60 mV from a holding potential of −30 mV and appeared unaltered by Gem expression. I_M amplitude was determined as the current deactivating during the 0.5-s pulse and normalized to cell membrane capacitance. Mean I_M density (Fig. 4D) and modulation by OXO-M (Fig. 4E) were not significantly affected by injection of Gem cDNA. These results suggest that the ability of Gem to depress I_{Ca} density does not arise from a general suppression of ion channel function.

To further analyze the physiological role of Gem, we examined the effect of wild-type Gem and various Gem mutants in PC12 cells in which Ca^{2+} influx through L-type calcium channels triggers GH secretion. As shown in Fig. 5, the effect of Gem on Ca^{2+}-stimulated secretion mostly paralleled the results observed in direct measurements of channel activity. Wild-type Gem inhibited secretion. GemS89N, which has reduced affinity for GTP (data not shown), failed to inhibit secretion. GemW269G partially inhibited secretion, and GemS261A inhibited secretion to the same extent as wild type. It was not possible to evaluate GemS289A in PC12 cells, because the Gem mutant protein was particularly unstable in this cell type (Fig. 5, Gem expression, bottom panel). Together

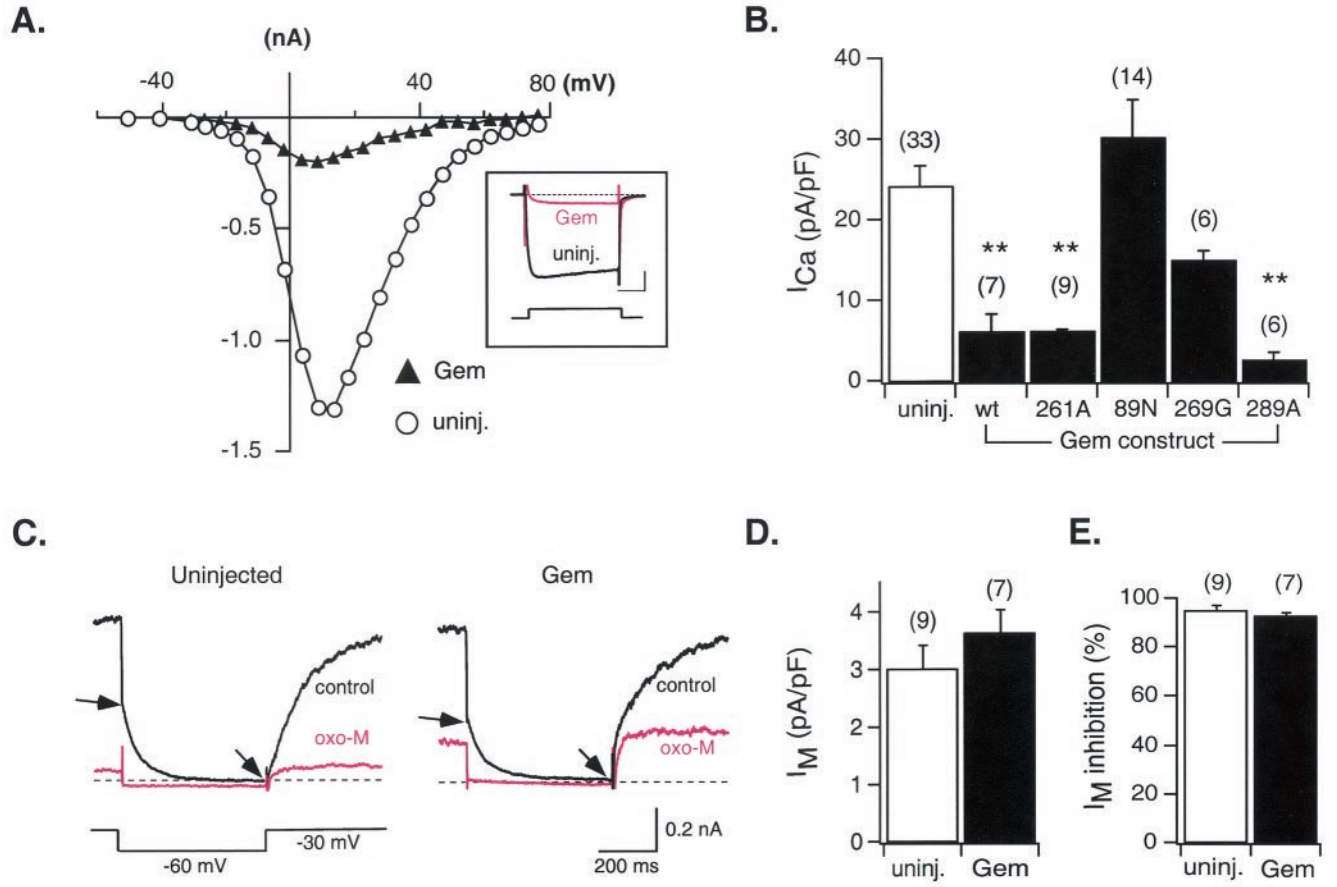

FIG. 4. Effects of heterologous Gem expression on N-type Ca^{2+} and M-type K^+ channels of sympathetic neurons. (A) Current-voltage relationships for Ca^{2+} currents (I_{Ca}) recorded from a control neuron (uninjected; open circles) and one injected approximately 24 h earlier with Gem cDNA (filled triangles). The inset illustrates superimposed I_{Ca} traces evoked by a 70-ms voltage step to +13 mV from a holding potential of −80 mV. Calibration bars, 20 ms (horizontal) and 0.3 nA (vertical). (B) Average I_{Ca} density (± SEM) in uninjected neurons (open bar) and neurons injected with wild-type (wt) or mutant Gem cDNA (filled bars) as indicated. I_{Ca} density was calculated from the I_{Ca} amplitude at a test pulse of +10 mV normalized to cell membrane capacitance. (C) Representative current traces of the K^+ current arising from M-type channels (I_M) recorded from a control neuron (left) and a neuron previously injected with Gem cDNA (right) in the absence (control) or presence of 10 μM OXO-M. I_M amplitude was measured as the difference in current magnitude between the beginning and end of a 500-ms hyperpolarizing voltage step to −60 mV (arrows). (D) Average I_M density (± SEM) measured from control neurons (open bar) and neurons previously injected with Gem cDNA (filled bar). I_M density was determined by normalizing I_M amplitude (see above) to membrane capacitance. (E) Average percent inhibition (± SEM) of I_M produced following OXO-M (10 μM) application in control neurons (open bar) and neurons previously injected with Gem cDNA (filled bar). Number of neurons tested is shown in parentheses. **, $P < 0.01$.

these data show that the cytoskeletal reorganization function of Gem does not play a role in Ca^{2+}-triggered secretion, despite the obvious role of the cytoskeleton in exocytosis.

14-3-3 binding increases the half-life of the Gem protein. We observed that GemS289A and GemS23A usually were expressed at lower steady-state levels than wild-type Gem. We hypothesized that 14-3-3-bound Gem may be "locked" into a more stable conformation compared to the nonbound form. We compared the half-lives of wild-type Gem and GemS23A after cycloheximide inhibition of new protein synthesis. As shown in Fig. 6, GemS23A was degraded approximately twice as rapidly as wild-type Gem, with a half-life of about 2 h. The half-life of GemS289A was similarly decreased (data not shown).

Phosphorylation of serines 289 and 261 can be observed using phosphopeptide-specific antibodies. Antisera were produced following immunization of rabbits with peptide containing phosphoserine 289. After affinity purification, such antisera appeared to be specific for Gem containing phosphorylated serine 289. Reactivity with anti–pS-289 was lost in phosphatase-treated lysates (data not shown). Antisera were reactive with wild-type Gem, but not Gem in which serine 289 had been replaced by an alanine or aspartic acid (Fig. 7A). The use of the GemS23A mutant that does not bind 14-3-3 revealed that 14-3-3 most likely protects serine 289 from dephosphorylation by cellular phosphatases (Fig. 7B). The relative level of serine 289 phosphorylation was greater in wild type compared to 14-3-3 binding-deficient GemS23A harvested in lysis buffer containing phosphatase inhibitors. In addition, serine 289 phosphorylation was greater for GemS23A isolated in the presence of the protein phosphatase 1 (PP1) and PP2A inhibitor calyculin A, compared to phosphorylation in its absence. These data imply that 14-3-3 binding prevents dephosphorylation of serine 289 by either PP1 or PP2A. It is also possible that

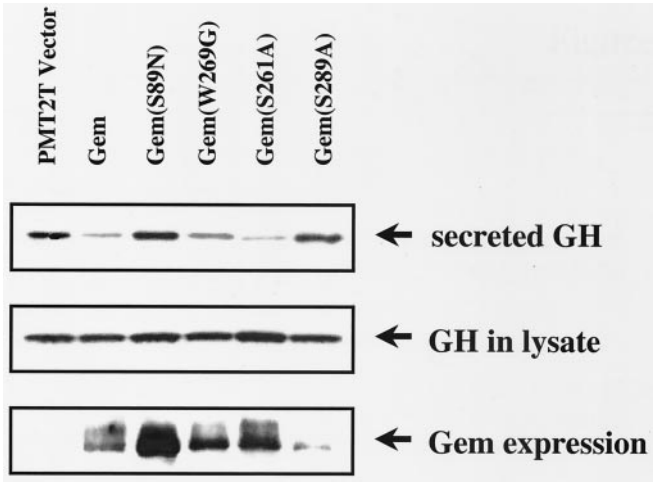

FIG. 5. Phosphorylation of Ser 261 is not required for Gem-mediated inhibition of Ca^{2+}-dependent GH secretion in PC12 cells, whereas mutation of serine 89 results in loss of Gem activity. Secretion of GH was stimulated by addition of high $[K^+]$ to PC12 cells cotransfected with human GH and empty vector or Gem cDNA. Secreted GH was detected in the supernatant by Western blotting using anti-hGH polyclonal antibody. Total GH and Gem expression were determined by Western analysis of cell lysates. Results shown are representative of at least nine independent experiments.

phosphorylation at serine 23 affects the efficiency of phosphorylation at serine 289.

Antisera directed against a peptide containing phosphoserine 261 were produced as well. Western blot analysis using affinity-purified antisera demonstrated a loss of reactivity to Gem in phosphatase-treated lysates (data not shown). There was no reactivity toward Gem in which serine 261 had been replaced by alanine or aspartic acid (Fig. 7A). Interestingly, there was reduced phosphorylation of serine 261 in the absence of serine 289 phosphorylation, as anti–pS-261 reacted weakly with GemS289A and GemS289D compared to wild-type Gem. These data suggest that there could be a requirement for the order of phosphorylation, with serine 289 preceding serine 261.

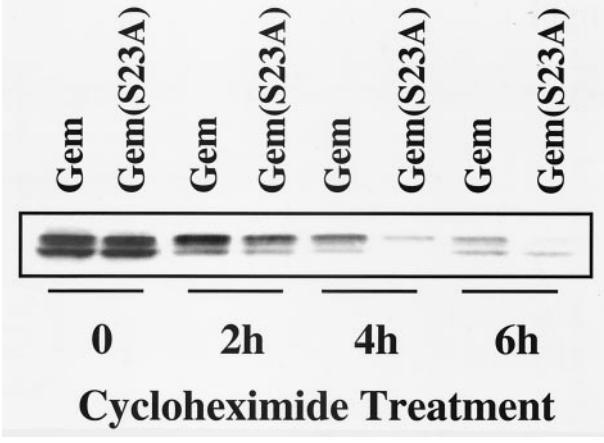

FIG. 6. Binding of 14-3-3 to Gem protects it from degradation. Cos-7 cells transfected with wild-type Gem or the 14-3-3-nonbinding mutant, GemS23A, were treated with cycloheximide (10 μg/ml) for 0 to 6 h. Gem protein levels were determined by Western blotting using anti-Gem polyclonal antibody.

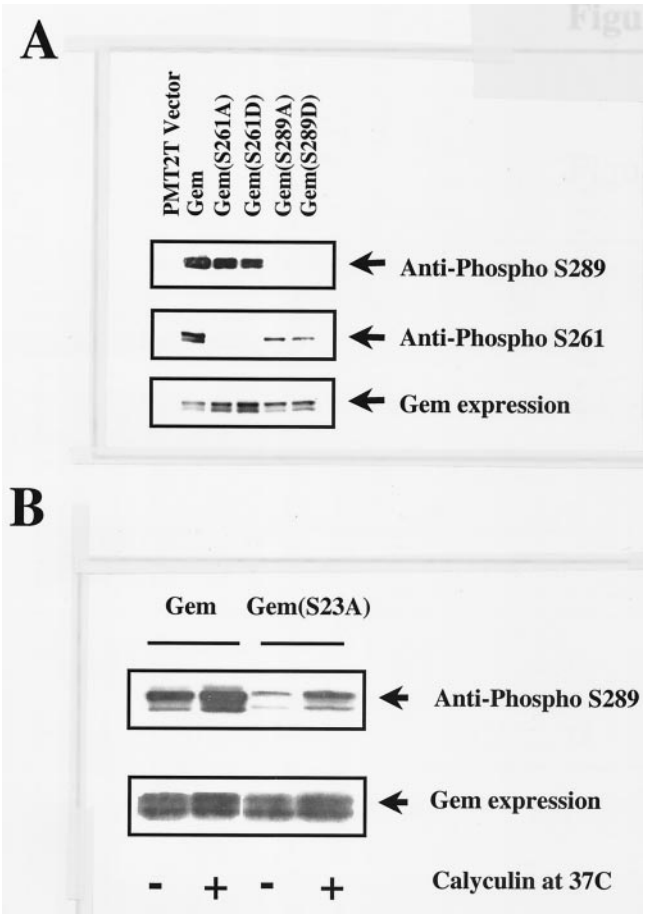

FIG. 7. (A) Highly specific antiphosphopeptide antibodies can distinguish between phosphorylated serines at positions 261 and 289. (B) In the GemS23A mutant that does not bind 14-3-3, phosphorylation of serine residue 289 is greatly reduced. Addition of calyculin A protects serine 289 from dephosphorylation. Lysates were prepared from Cos-7 cells transfected with wild-type Gem or Gem mutants. Phosphorylation of serines 261 and 289 was detected following immunoprecipitation with Gem monoclonal antibody P2D10 followed by Western blotting using antiphosphopeptide antibodies. Total Gem expression was determined using anti-Gem polyclonal antibody.

To determine the phosphorylation status of serines 261 and 289 in endogenous Gem, we assayed reactivity of the anti–pS-261 and –pS-289 peptide antibodies toward Gem induced by T-cell receptor activation in normal peripheral blood T cells. As shown in Fig. 8, Gem was induced and accumulated with time after mitogenic activation of T cells. Phosphorylation of serines 261 and 289 could be observed at the earliest time point of Gem protein expression. Serine 261 phosphorylation appeared to reach peak expression with slightly delayed kinetics relative to serine 289.

Gem Ser 261 phosphorylation occurs downstream of PKCζ activation. We used protein kinase inhibitors in combination with anti–pS-289 antibodies to screen for the kinases responsible for phosphorylation of serine 289 in N1E-115 or Cos cells transfected with GemS23A. GemS23A was used in order to reveal dynamic dephosphorylation of serine 289, which is prob-

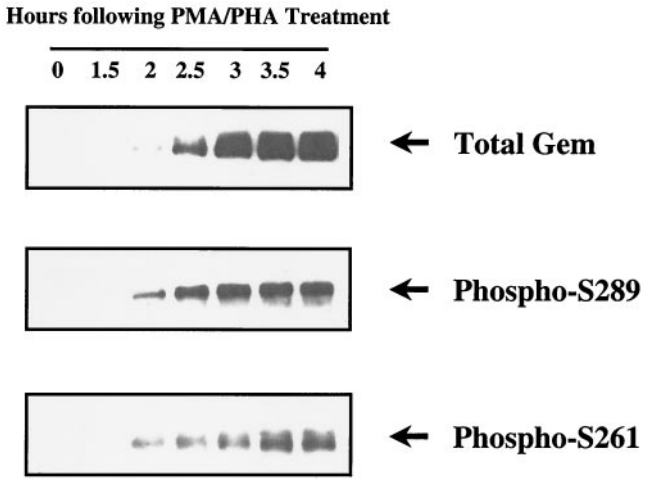

FIG. 8. Phosphorylation of serines 261 and 289 in endogenous Gem, expressed in peripheral blood T cells following mitogenic stimulation. Human T cells were treated with phorbol myristate acetate (20 ng/ml) and phytohemagglutinin (5 μg/ml). Total Gem expressed and phosphorylation of serines 261 and 289 were determined at each time interval using Western blot analysis as described in the legend for Fig. 7.

ably inaccessible to phosphatases following 14-3-3 binding. The list of inhibitors used to examine potential kinases responsible for phosphorylation of serine 289 is shown in Table 1. None of the drugs employed appeared to inhibit serine 289 phosphorylation under the conditions that were used (data not shown). The context of serine 289, amino acid sequence SCHD, is a potential target site for casein kinase II, but apigenin, a casein kinase II inhibitor, did not diminish phosphorylation at serine 289. This suggests that a separate class of enzymes from those tested are responsible for phosphorylation of serine 289 or, more likely, that more than one kinase phosphorylates serine 289 in Cos cells.

Using a similar strategy, we found that phosphorylation of Ser 261 in wild-type Gem was inhibited in the presence of micromolar concentrations of Go6850, but not Go6979, suggesting that an atypical PKC (aPKC) might be involved in the pathway (2) (Fig. 9A). These results were supported by cotransfection experiments showing that wild-type or constitutively activated PKCζ greatly increased pS-261 reactivity (Fig. 9B). A well-studied pathway leading to aPKC activation is the PI-3 kinase/PDK-1 pathway. However, phosphorylation of Ser 261 was not reduced following treatment with the PI 3-kinase inhibitor LY294002 but, surprisingly, appeared to increase (Fig. 9A). In addition, phosphorylation of Ser 261 was unaffected following cotransfection of either a mutant PI-3 kinase p85 subunit (p85Δ479-513) that constitutively inhibits activa-

TABLE 1. Inhibitors used to screen for protein kinase-dependent pS-289 phosphorylation

Inhibitor	Concn (μM)	Target[a]
LY294002	25	PI3K
Go6976	0.02, 1, 10	PKCα, PKCβ1
Go6850	10, 20	PKC including ζ
H9 dihydrochloride	1, 10	PKA
H9 dihydrochloride	200	PKC
KT5720	0.3, 1, 10	PKA
KT5823	1, 2	PKG
Y27632	10	Rok
PD98059	50	Mek
Apigenin	20, 80	CK2
KN93	1, 10, 30	CAM kinase II
W7	1, 10, 30	CaMK, MLCK

[a] Abbreviations: PI3K, PI 3-kinase; CAM, calmodulin-dependent; CaMK, calmodulin-dependent kinase; MLCK, myosin light-chain kinase.

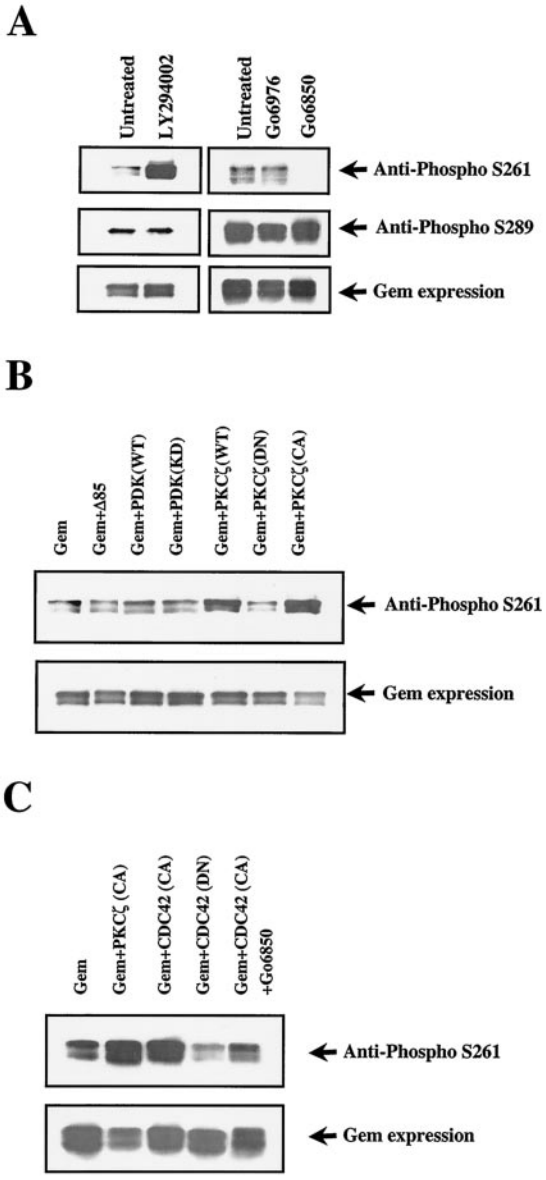

FIG. 9. (A) Gem Ser261 phosphorylation is reduced following treatment with an inhibitor of aPKCs. Cos-7 cells were transfected with wild-type Gem and either left untreated or exposed to Go6976 (20 nM, shown here) or Go6850 (10 μM). Cells were also treated with the PI 3-kinase inhibitor LY294002 (25 μM). (B) Gem Ser261 phosphorylation is stimulated by coexpression of wild-type or constitutively active PKCζ. Cos cells were cotransfected with wild-type Gem and other plasmids as indicated. The expression of proteins coexpressed with Gem was verified by Western blotting with appropriated antibodies (data not shown).

tion of the p110 catalytic subunit or a dominant-negative form of PDK-1 (Fig. 9B). Therefore, it appears that PKCζ-dependent phosphorylation of Gem 261 is not downstream of PI-3 kinase/PDK-1 in Cos cells.

Another pathway that is important for establishing cellular polarity results from the cdc42-dependent activation of PKCζ in complex with PAR6 (8). As shown in Fig. 9C, coexpression of constitutively activated cdc42 resulted in increased S261 phosphorylation of Gem, which was inhibited by Go6850 treatment, suggesting that cdc42-stimulated PKCζ activation leads to Gem 261 phosphorylation. Constitutively activated rac did not result in a similar increase in Gem S261 phosphorylation (data not shown). Consistent with a role for the cdc42 pathway in GemS261 phosphorylation, dominant-negative cdc42 partially inhibited phosphorylation of constitutively expressed Gem.

DISCUSSION

We have shown here that Gem has at least two functional pathways that are regulated by distinct structural modifications. First, phosphorylation of serines 261 and 289, located in the COOH-terminal extension of Gem outside the ras core and previously defined ROKβ interaction region, are required for ROKβ-mediated cytoskeletal function. We hypothesize that these phosphorylations within the COOH terminus lead to a conformational change required for the ROKβ-dependent Gem function. Second, inhibition of voltage-gated Ca^{2+} channel activity is regulated by GTP and possibly by calmodulin binding to Gem.

Gem inhibition of high-voltage-activated (HVA) Ca^{2+} channel activity is most likely mediated through an interaction with the HVA Ca^{2+} auxiliary β subunit isoforms. The finding that M-type K^+ channels are unaffected by Gem expression is consistent with this notion and rules out a general nonspecific suppression of ion channel function. The in vitro interaction of Gem with the β subunit previously has been shown to be dependent upon GTP loading of Gem (3), and the demonstration here that the GTP-binding mutant GemS89N has no functional activity is consistent with the notion that GTP binding regulates the β subunit-Gem interaction. HVA Ca^{2+} channel inhibition appears similar to a classical small GTPase effector pathway in that GTP binding is required, although the GTPase activity of Gem is unlikely, based upon sequence comparisons to known GTPases. Defining a mechanism for regulating GDP-GTP exchange on Gem is an important question yet to be answered.

In addition, unique regulatory mechanisms such as calmodulin binding exist for Gem and other RGK family members (12, 20). Calmodulin binding in the C-terminal extension of Gem is required for maximal inhibition of HVA Ca^{2+} channels by ectopically expressed Gem, as determined by measurement of electrical activity in primary neurons and by Ca^{2+}-evoked secretion in PC12 cells (Fig. 4 and 5) (3). The suggestion has been made that Gem inhibits HVA Ca^{2+} channel activity as a result of sequestering the β subunit and thereby inhibiting transport of the α subunit to the cell surface. However, the relatively fast kinetics of virtually complete inhibition within 20 h suggest that a direct action of Gem upon the cell surface-localized channel should be considered.

The second functional property of Gem, Rad, and Rem is their stimulation of cytoskeletal reorganization (16, 22, 23, 30). As shown here, the cytoskeletal function of Gem, mediated by an inhibition of ROKβ, is regulated by phosphorylations at serines 289 and 261 in the C-terminal extension of Gem. Mutation of either serine 261 or 289 to alanine resulted in a loss of Gem function in stimulating neurite extension, inhibiting focal adhesion formation, or reversing ROKβ-mediated neurite retraction (Fig. 2). Mutation of the same serines to aspartic acids, which potentially mimic phosphoserine structure, did not disrupt these cytoskeletal functions. We have found no evidence that phosphorylation of either serine 261 or 289 alters the subcellular distribution of Gem (data not shown). The interaction of Gem with ROKβ has been mapped to the core region of Gem in yeast two-hybrid analyses (30). Phosphorylation of serines 261 and 289 most likely leads to a conformational change in Gem, revealing binding sites for ROKβ or other interacting proteins mediating the ROKβ-dependent function of Gem. The in vivo interaction of Gem and ROKβ is not of sufficiently high affinity to definitively address this question with coprecipitation analyses.

14-3-3 binding to Gem occurs as a result of bidentate binding to phosphoserine 23 in the N-terminal extension and phosphoserine 289 in the C-terminal extension. Although phosphorylation of serine 289 is required for cytoskeletal reorganization, subsequent 14-3-3 binding is not required as evidenced by the retention of activity in GemS23A and GemS289D mutants. Perhaps a conformational change stimulated by serine 289 phosphorylation is sufficient for activity of overexpressed Gem. As shown in Fig. 7B, 14-3-3 binding partially protects phosphoserine 289 from dephosphorylation. In addition, 14-3-3 dimers are rigid structures which are believed to lock their binding partners into specific conformations (31). 14-3-3-bound Gem has a twofold-longer half-life than nonbound Gem (Fig. 6). A similar increase in protein stability following 14-3-3 binding has been described for the Wee1 kinase (29). We expect that the role of 14-3-3 in maintaining an active conformation for Gem and/or regulating the level of Gem protein could be quite significant under conditions where Gem is limiting. Gem protein levels are subject to rapid fluctuations as a result of transcriptional control of Gem mRNA production and a short protein half-life (17). Under such conditions, phosphorylation of serine 289 and 14-3-3 association may indirectly regulate HVA Ca^{2+} channels through modulating the cellular concentration of Gem.

The combined use of PKC inhibitors and phosphopeptide-specific antibodies has revealed a role for aPKCs in GemS261 phosphorylation. In addition, in Cos cells it appears that stimulation of PKCζ through cdc42 activation leads to GemS261 phosphorylation, but stimulation of PKCζ through PI-3 kinase activation does not. The availability of Gem for PKCζ-dependent phosphorylation most likely is dependent upon appropriate localization of both proteins via scaffolding complexes within the cell. The biochemical mechanism whereby cdc42 activates PKCζ in the context of PAR6 has not been established (8). cdc42 is important for orienting actin polymerization at the leading edge of migrating cells (18), and cdc42 in conjunction with PKCζ, PAR6, and PAR3 is important in determining cell polarity (8). Activation of aPKCs has been shown to result in depolymerization of actin stress fibers down-

stream of cdc42 activation (6). Thus, the regulation of Gem by PKCζ-dependent phosphorylation of S261, leading to Gem inhibition of ROKβ function, is consistent with a regulatory circuit that segregates actin polymerization and stress fiber formation.

REFERENCES

1. **Aresta, S., M. F. de Tand-Heim, F. Beranger, and J. de Gunzburg.** 2002. A novel Rho GTPase-activating-protein interacts with Gem, a member of the Ras superfamily of GTPases. Biochem. J. **367:**57–65.
2. **Baier-Bitterlich, G., F. Uberall, B. Bauer, F. Fresser, H. Wachter, H. Grunicke, G. Utermann, A. Altman, and G. Baier.** 1996. Protein kinase C-θ isoenzyme selective stimulation of the transcription factor complex AP-1 in T lymphocytes. Mol. Cell. Biol. **16:**1842–1850.
3. **Beguin, P., K. Nagashima, T. Gonoi, T. Shibasaki, K. Takahashi, Y. Kashima, N. Ozaki, K. Geering, T. Iwanaga, and S. Seino.** 2001. Regulation of Ca^{2+} channel expression at the cell surface by the small G-protein kir/Gem. Nature **411:**701–706.
4. **Bourne, H. R., D. A. Sanders, and F. McCormick.** 1991. The GTPase superfamily: conserved structure and molecular mechanism. Nature **349:**117–127.
5. **Chen, H., F. H. Nystrom, L. Q. Dong, Y. Li, S. Song, F. Liu, and M. J. Quon.** 2001. Insulin stimulates increased catalytic activity of phosphoinositide-dependent kinase-1 by a phosphorylation-dependent mechanism. Biochemistry **40:**11851–11859.
6. **Coghlan, M. P., M. M. Chou, and C. L. Carpenter.** 2000. Atypical protein kinases Cλ and -ζ associate with the GTP-binding protein Cdc42 and mediate stress fiber loss. Mol. Cell. Biol. **20:**2880–2889.
7. **Cohen, L., R. Mohr, Y. Y. Chen, M. Huang, R. Kato, D. Dorin, F. Tamanoi, A. Goga, D. Afar, N. Rosenberg, et al.** 1994. Transcriptional activation of a ras-like gene (kir) by oncogenic tyrosine kinases. Proc. Natl. Acad. Sci. USA **91:**12448–12452.
8. **Etienne-Manneville, S., and A. Hall.** 2003. Cell polarity: Par6, aPKC and cytoskeletal crosstalk. Curr. Opin. Cell Biol. **15:**67–72.
9. **Finlin, B. S., and D. A. Andres.** 1999. Phosphorylation-dependent association of the Ras-related GTP-binding protein Rem with 14-3-3 proteins. Arch. Biochem. Biophys. **368:**401–412.
10. **Finlin, B. S., and D. A. Andres.** 1997. Rem is a new member of the Rad- and Gem/Kir Ras-related GTP-binding protein family repressed by lipopolysaccharide stimulation. J. Biol. Chem. **272:**21982–21988.
11. **Finlin, B. S., H. Shao, K. Kadono-Okuda, N. Guo, and D. A. Andres.** 2000. Rem2, a new member of the Rem/Rad/Gem/Kir family of Ras-related GTPases. Biochem. J. **347:**223–231.
12. **Fischer, R., Y. Wei, J. Anagli, and M. W. Berchtold.** 1996. Calmodulin binds to and inhibits GTP binding of the ras-like GTPase Kir/Gem. J. Biol. Chem. **271:**25067–25070.
13. **Hamill, O. P., A. Marty, E. Neher, B. Sakmann, and F. J. Sigworth.** 1981. Improved patch-clamp techniques for high-resolution current recording from cells and cell-free membrane patches. Pflugers Arch. **391:**85–100.
14. **Ikeda, S. R.** 1997. Heterologous expression of receptors and signaling proteins in adult mammalian sympathetic neurons by microinjection. Methods Mol. Biol. **83:**191–202.
15. **Ikeda, S. R., D. M. Lovinger, B. A. McCool, and D. L. Lewis.** 1995. Heterologous expression of metabotropic glutamate receptors in adult rat sympathetic neurons: subtype-specific coupling to ion channels. Neuron **14:**1029–1038.
16. **Leone, A., N. Mitsiades, Y. Ward, B. Spinelli, V. Poulaki, M. Tsokos, and K. Kelly.** 2001. The Gem GTP-binding protein promotes morphological differentiation in neuroblastoma. Oncogene **20:**3217–3225.
17. **Maguire, J., T. Santoro, P. Jensen, U. Siebenlist, J. Yewdell, and K. Kelly.** 1994. Gem: an induced, immediate early protein belonging to the Ras family. Science **265:**241–244.
18. **Meili, R., and R. A. Firtel.** 2003. Two poles and a compass. Cell **114:**153–156.
19. **Miller, R. T., S. B. Masters, K. A. Sullivan, B. Beiderman, and H. R. Bourne.** 1988. A mutation that prevents GTP-dependent activation of the alpha chain of Gs. Nature **334:**712–715.
20. **Moyers, J. S., P. J. Bilan, J. Zhu, and C. R. Kahn.** 1997. Rad and Rad-related GTPases interact with calmodulin and calmodulin-dependent protein kinase II. J. Biol. Chem. **272:**11832–11839.
21. **Pai, E. F., U. Krengel, G. A. Petsko, R. S. Goody, W. Kabsch, and A. Wittinghofer.** 1990. Refined crystal structure of the triphosphate conformation of H-ras p21 at 1.35 Å resolution: implications for the mechanism of GTP hydrolysis. EMBO J. **9:**2351–2359.
22. **Pan, J. Y., W. E. Fieles, A. M. White, M. M. Egerton, and D. S. Silberstein.** 2000. Ges, a human GTPase of the Rad/Gem/Kir family, promotes endothelial cell sprouting and cytoskeleton reorganization. J. Cell Biol. **149:**1107–1116.
23. **Piddini, E., J. A. Schmid, R. de Martin, and C. G. Dotti.** 2001. The Ras-like GTPase Gem is involved in cell shape remodelling and interacts with the novel kinesin-like protein KIF9. EMBO J. **20:**4076–4087.
24. **Quon, M. J., H. Chen, B. L. Ing, M. L. Liu, M. J. Zarnowski, K. Yonezawa, M. Kasuga, S. W. Cushman, and S. I. Taylor.** 1995. Roles of 1-phosphatidylinositol 3-kinase and ras in regulating translocation of GLUT4 in transfected rat adipose cells. Mol. Cell. Biol. **15:**5403–5411.
25. **Ravichandran, L. V., D. L. Esposito, J. Chen, and M. J. Quon.** 2001. Protein kinase C-zeta phosphorylates insulin receptor substrate-1 and impairs its ability to activate phosphatidylinositol 3-kinase in response to insulin. J. Biol. Chem. **276:**3543–3549.
26. **Reynet, C., and C. R. Kahn.** 1993. Rad: a member of the Ras family overexpressed in muscle of type II diabetic humans. Science **262:**1441–1444.
27. **Stamnes, M.** 2002. Regulating the actin cytoskeleton during vesicular transport. Curr. Opin. Cell Biol. **14:**428–433.
28. **Standaert, M. L., L. Galloway, P. Karnam, G. Bandyopadhyay, J. Moscat, and R. V. Farese.** 1997. Protein kinase C-zeta as a downstream effector of phosphatidylinositol 3-kinase during insulin stimulation in rat adipocytes. Potential role in glucose transport. J. Biol. Chem. **272:**30075–30082.
29. **Wang, Y., C. Jacobs, K. E. Hook, H. Duan, R. N. Booher, and Y. Sun.** 2000. Binding of 14-3-3β to the carboxyl terminus of Wee1 increases Wee1 stability, kinase activity, and G_2-M cell population. Cell Growth Differ. **11:**211–219.
30. **Ward, Y., S. F. Yap, V. Ravichandran, F. Matsumura, M. Ito, B. Spinelli, and K. Kelly.** 2002. The GTP binding proteins Gem and Rad are negative regulators of the Rho-Rho kinase pathway. J. Cell Biol. **157:**291–302.
31. **Yaffe, M. B.** 2002. How do 14-3-3 proteins work? Gatekeeper phosphorylation and the molecular anvil hypothesis. FEBS Lett. **513:**53–57.
32. **Zhu, J., P. J. Bilan, J. S. Moyers, D. A. Antonetti, and C. R. Kahn.** 1996. Rad, a novel Ras-related GTPase, interacts with skeletal muscle beta-tropomyosin. J. Biol. Chem. **271:**768–773.